frontiers | Frontiers in Earth Science

TYPE Original Research
PUBLISHED 13 January 2023
DOI 10.3389/feart.2022.1082439

OPEN ACCESS

EDITED BY
Dadong Liu,
China University of Petroleum, Beijing, China

REVIEWED BY
Zhipeng Huo,
Northeastern University at Qinhuangdao, China
Yingchun Guo,
Chinese Academy of Geologi-cal Sciences (CAGS), China

*CORRESPONDENCE
Lei Gong,
kcgonglei@foxmail.com

SPECIALTY SECTION
This article was submitted to Structural Geology and Tectonics, a section of the journal Frontiers in Earth Science

RECEIVED 28 October 2022
ACCEPTED 22 November 2022
PUBLISHED 13 January 2023

CITATION
Mi L, Fan T, Fan H, Niu T, Gong L, Su X, Sun Y and Cheng Y (2023), Fracture development and controlling factors at metamorphic buried-hill reservoirs of Bozhong 19-6 gas field in Bohai Bay, East China.
Front. Earth Sci. 10:1082439.
doi: 10.3389/feart.2022.1082439

Fracture development and controlling factors at metamorphic buried-hill reservoirs of Bozhong 19-6 gas field in Bohai Bay, East China

Lijun Mi[1], Tingen Fan[1], Hongjun Fan[1], Tao Niu[1], Lei Gong[2]*, Xiaocen Su[2], Yonghe Sun[2] and Yuqi Cheng[2]

[1]CNOOC Research Institute Ltd., Beijing, China, [2]Bohai-Rim Energy Research Institute, Northeast Petroleum University, Qinhuangdao, China

Fractures of multi-scales and multi-origins are primary storage space and effective seepage channels for metamorphic buried-hill reservoirs. They not only allow communication between various pores to enhance storage and seepage capacity, but also are essential for high yields. Fracture development and controlling factors at metamorphic buried-hill reservoirs of Bozhong 19-6 Gas Field were investigated based on imaging log, core data, experiments, e.g., thin sections and scanning electron microscope, and outcrop description. Results show that structural fractures, weathering fractures and dissolution fractures were developed in the metamorphic buried-hill reservoirs in the study area, among which structural fractures and weathering fractures are the most popular ones. However, fracture types varied obviously among different structure positions. Lithology, fault, weathering crust and ancient landform are primary factors affecting fracture distribution. Fractures were prone to be developed at lithology with high bright mineral contents. Faults were characterized by a dual structure including fault core and damage zone. Fracture density followed a decreasing trend with increasing distance from faults. Damage zone could be identified when fracture density was consistent with regional fracture density. The width of the damage zone was determined by factors such as fault scale and structure location. Well-connected weathering fractures were popular at the leached unit, with structural fractures of secondary importance. The unweathered unit was dominated by structural fractures with low density.

KEYWORDS

metamorphic buried-hill, fractures, developmental characteristics, controlling factors, Bozhong 19-6

Introduction

Continuing oil and gas exploration activities at deep and ultra deep basins have made buried-hill reservoirs important exploration targets in recent years (Hou et al., 2013; Wang et al., 2015; Zhou et al., 2022). A large number of buried-hill reservoirs have been discovered in metamorphic rocks or granite basement at Baihu Oilfield in Vietnam and Bongor Basin in Chad (Dou et al., 2015; Wang et al., 2019; Luo et al., 2020; Luo et al., 2021; Zhou et al., 2022). Recently, major breakthroughs have also been made at the Archeozoic metamorphic buried-hill reservoirs at the Bohai Bay Basin, China, e.g., reserves of 100 million tons have been discovered at Jinzhou 25-1 metamorphic buried-hill, Xinglongtai buried hill at Liaohe Basin and Bozhong 19-6 metamorphic buried hill (Luo et al., 2014; Luo et al., 2016; Wang et al., 2019; Xu et al., 2020; Ye et al., 2021). Multiple types of buried-hill reservoirs were developed in petroliferous basins, where a large number of structural fractures and weathering fractures grew due to multi-stage tectonic movements and long-term weathering. These fractures were developed into complex fracture networks, complicating structure of metamorphic buried-hill reservoirs with strong heterogeneity (Luo et al., 2014; Xu et al., 2020; Ye et al., 2021). As a result, oil and gas enrichment was not only controlled by lithologies and reservoir properties, etc., but also was directly determined by fracture development [(Zhou et al., 2022)· (Zhou et al., 2005; Luo et al., 2014; Deng, 2015; Luo et al., 2016; Hu et al., 2017; Zhou et al., 2017; Xu et al., 2020; Fan et al., 2021; Ye et al., 2021)]. Previous studies show that natural fractures can not only provide storage space for oil and gas accumulation at metamorphic buried-hill reservoirs, but also are effective seepage channels (Gao et al., 2015; Gong et al., 2016), since they not only communicate pores and enhance permeability of metamorphic buried-hill reservoirs, but also govern high yields (Huang et al., 2016; Hu et al., 2017; Xue et al., 2020). However, as suggested by increasing exploration and development activities, fracture characteristics and development mechanism at buried-hill reservoirs as well as primary controlling factors are poorly understood (Zeng et al., 2016; Chen et al., 2018), which brings considerable challenge for fracture distribution prediction and exerts significantly negative impact on drilling and reservoir development (Gong et al., 2017). Taking metamorphic buried-hill reservoirs at Bozhong 19-6 Gas Field as an example, this paper used imaging log, core data, and experiments, e.g., thin sections and scanning electron microscope (SEM) images, etc., to investigate genetic types and distribution of fractures in metamorphic reservoirs. After that, primary controlling factors of fractures development at metamorphic buried-hill reservoirs were analyzed based on weathering crust and fault system on outcrops as well as fracture distribution under different landforms.

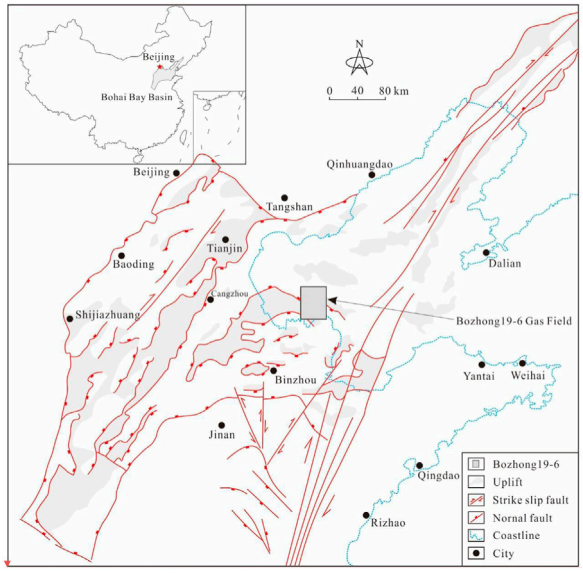

FIGURE 1
Structure location of Bozhong 19-6 Gas Field (Gong et al., 2019a).

Geological setting

Bozhong 19-6 Gas Field is located at the southwest of Bozhong Sag, bounded by Bozhong Sag, Shanan Sag and Huanghekou Sag. It is a faulted anticline complicated by strike slip faults and associated faults, with a structure pattern of "a high-in-sag" (Figure 1) (Dou et al., 2015; Xie, 2020; Xue et al., 2020; Fan et al., 2021). The strata drilled in Bozhong 19-6 Gas Field are: the Quaternary Pingyuan Formation, the Neogene Minghuazhen Formation and the Guantao Formation, the Paleogene Dongying Formation, the Shahejie Formation and the Kongdian Formation, and the Archaeozoic buried hill, from top to bottom. Drilling data shows that, except the Pingyuan Formation, hydrocarbon intervals are developed in all these Formations, with oil intervals at the shallow and gas intervals at the deep (Hou et al., 2019; Xu et al., 2019; Chen et al., 2021; Luo et al., 2021). The Archaeozoic buried hill is complicated in lithology, which can be divided into two types, i.e., metamorphic rocks and intrusive rocks, with six sub types. The metamorphic rocks can be further divided into regional metamorphic rocks, dynamic metamorphic rocks and migmatite. The regional metamorphic rocks include metamorphic granite and gneiss. The dynamic metamorphic rocks are cracked gneiss and cataclasite. The migmatite is primarily migmatite gneiss and migmatite granite. The magmatite can be divided into acidic intrusion-granite, intermediate intrusion-diorite porphyry and basic intrusion-diabase.

The metamorphic rocks are minerally composed of bright quartz, plagioclase and potassium feldspar. The feldspar and quartz account for 20.0%–100.0%, with an average of 91%. The dark minerals, mainly biotite, white mica, hornblende, with a small

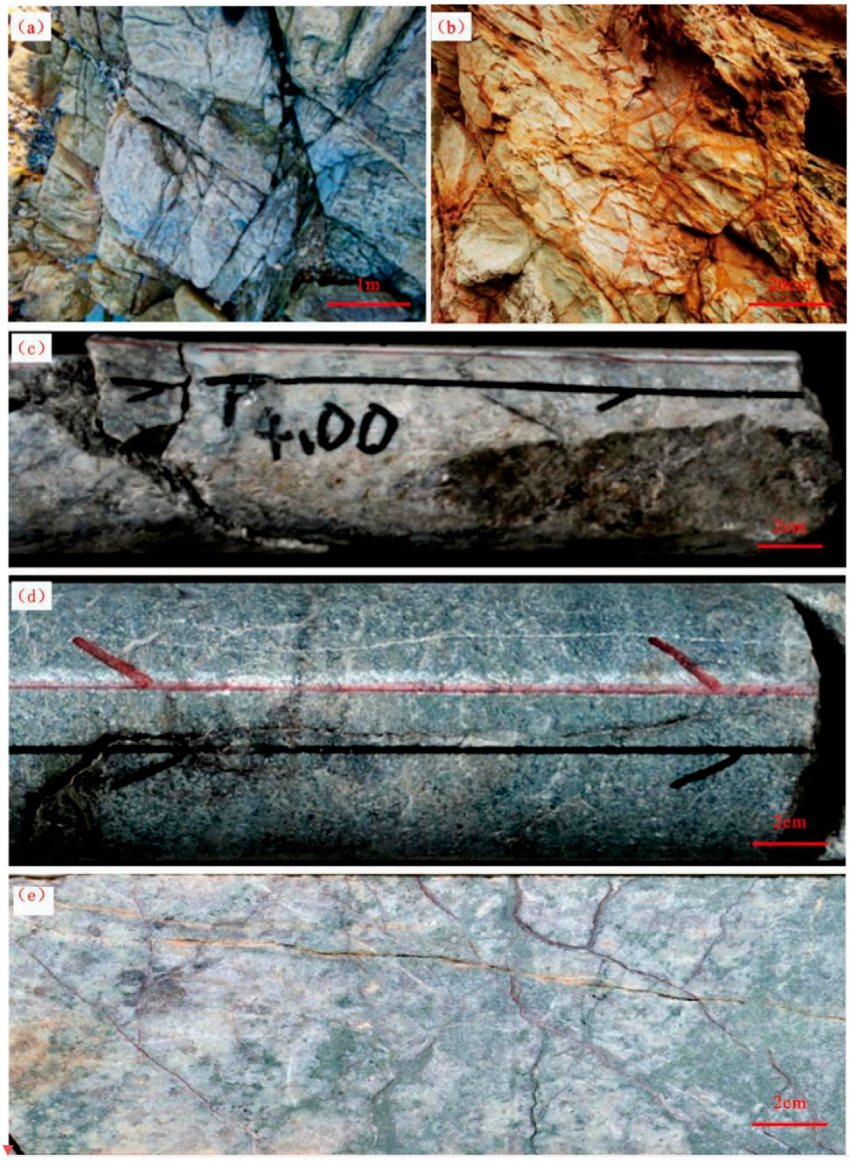

FIGURE 2
Fracture types and development characteristics in the study area. **(A)** Structural fractures. **(B)** Weathering fractures. **(C)** Shear fractures. **(D)** Extensional fracture. **(E)** Weathering fractures.

amount of siderite. Pyrite and ankerite, are low in content, between 5% and 15%, with an average of 9%. The buried-hill reservoirs are commonly dual media those are primarily composed of macro fractures, micro fractures, intergranular pores, intragranular solution pores, etc. (Zhou et al., 2022) They are primarily fractured-porous ones and porous-fractured ones, followed by fractured ones and porous ones. Core analysis shows that, the Archaeozoic buried hill is 0.8 %–15.8% in porosity, with an average of 6.4% and a median of 6.7%. The permeability ranges from 0.02 mD to 508.61 mD, with an average of 8.90 mD and a median of 0.24 mD. Log interpretation suggests, the porosity is 1.0%–25.8%, with an average of 4.5% and a median of 3.8%, and the permeability is between 0.003 mD and 696.10 mD, with an average of 4.24 mD and a median of 0.02 mD.

Fracture development

Fracture types and characteristics

Structural fractures, weathering fractures and dissolution fractures can be identified from the study area based on outcrops, imaging log, cores, thin sections and SEM images.

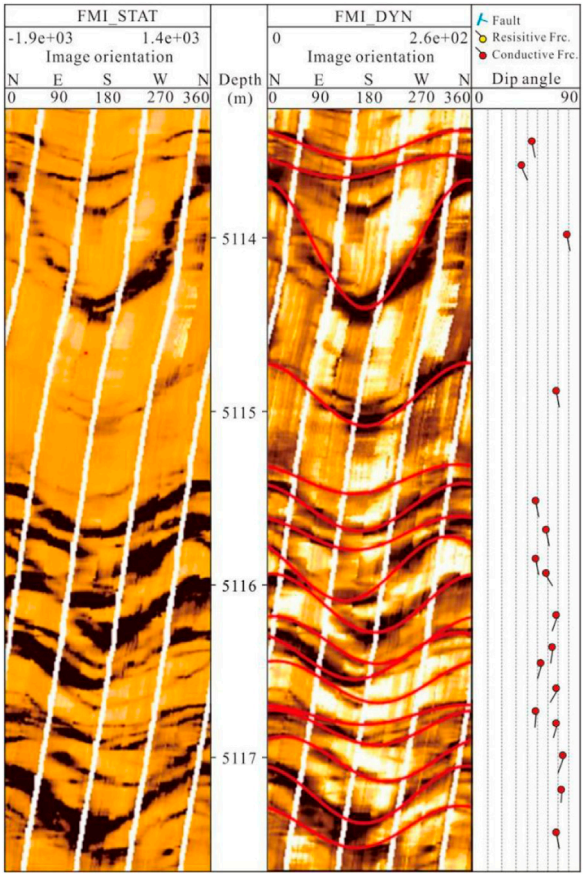

FIGURE 3
Fracture characteristics on imaging log.

Among them, structural fractures and weathering fractures are the primary ones, while some of them were dissolved to form dissolution fractures (Figure 2).

Structural fractures are referred to natural fractures derived from regional or local tectonic stress field, which are well developed in all kinds of metamorphic rocks and granites, with large scale and long extension. They are generally several meters to tens of meters in length, with the maximum up to hundreds of meters (Figure 2A). These fractures often appear in groups with obvious regularity and orientation but no obvious variation in occurrence. Structural fractures are the most popular ones in metamorphic reservoirs in the study area, which are characterized by multi-phases, multi-orientations, uneven development with various scales and filling behaviors. They can also be divided into shear fractures and extensional fractures based on their mechanical properties. Shear fractures, mainly oblique fractures and high-angle fractures, are generally conjugated in various lithologies with flat and smooth surfaces. Slips and steps can be observed in some samples, which are partly filled by calcite (Figure 2C). They are extended widely with large length, which can cut through several layers. Some shear fractures are slipped obviously (with displacement of 2–5 cm) to form small-scale faults with small fault cores, including structural lenses, breccias and fault gouges, etc. Extensional fractures have rough and uneven surfaces, which are often filled with minerals. They are irregularly distributed in the study area with high dip angle and small length (Figure 2D).

Weathering fractures are commonly extensional ones derived from physical or chemical weathering of exposed rocks, in honeycomb or network pattern with high density. However, they are irregularly distributed with bend or arc-shaped surface and unstable occurrence. These fractures are relatively small in extension, generally centimeter-scale to decimeter-scale with dip angles of 0–90°, but some can be up to meter-scale. They are commonly filled with clay minerals, or are contaminated by iron (oxidized to red) (Figures 2B,E). Dissolution fractures mainly occur along early weathering fractures and/or structural fractures, which widens fracture apertures and are accompanied by dissolution holes locally (Figure 3).

Quantitative fracture characterization

Two types of resistive fractures and conductive fractures were identified from imaging logs (Figure 3), among which conductive fractures (effective fractures) are the main ones (Figure 4A), indicating good fracture effectiveness. Imaging log interpretation suggests that fractures in the study area are complex in orientation, which are primarily extended along NE-SW, near E-W, near N-S and NW-SE trending (Figure 4B). Fracture orientation varies greatly among different structure positions, especially at the structure high, near faults and at fault intersections, where orientations are generally consistent with fault strikes. They are mainly oblique fractures with dip angle of 30°–60°, followed by bedding-parallel fractures and subvertical fractures (Figure 4C). The fracture density identified by imaging log is 1–5 m^{-1}, which is higher in the semi-weathered zone compared with unweathered zone (Figure 4D). However, multiple fractured units are also developed in the unweathered zone.

Core observations show that, the dip angle of fractures is distributed between 0° and 90°, with the peak value at 30°–70°. It varies significantly among different fracture types. e.g., 60°–90° for structural fractures, and 30°–60° for weathering fractures (Figure 5A). The fracture length on cores is about 5–15 cm, with an average of 9.39 cm and a maximum of 45 cm (Figure 5B). The structural fractures are large in length, generally about 12–20 cm, with an average of 17.09 cm. Different from that, weathering fractures are short, with length of 4–7 cm and an average of 5.81 cm. Fractures are popular on cores, especially in the weathering zone. The areal density of weathering fractures is about 30–70 m/m^2, with an

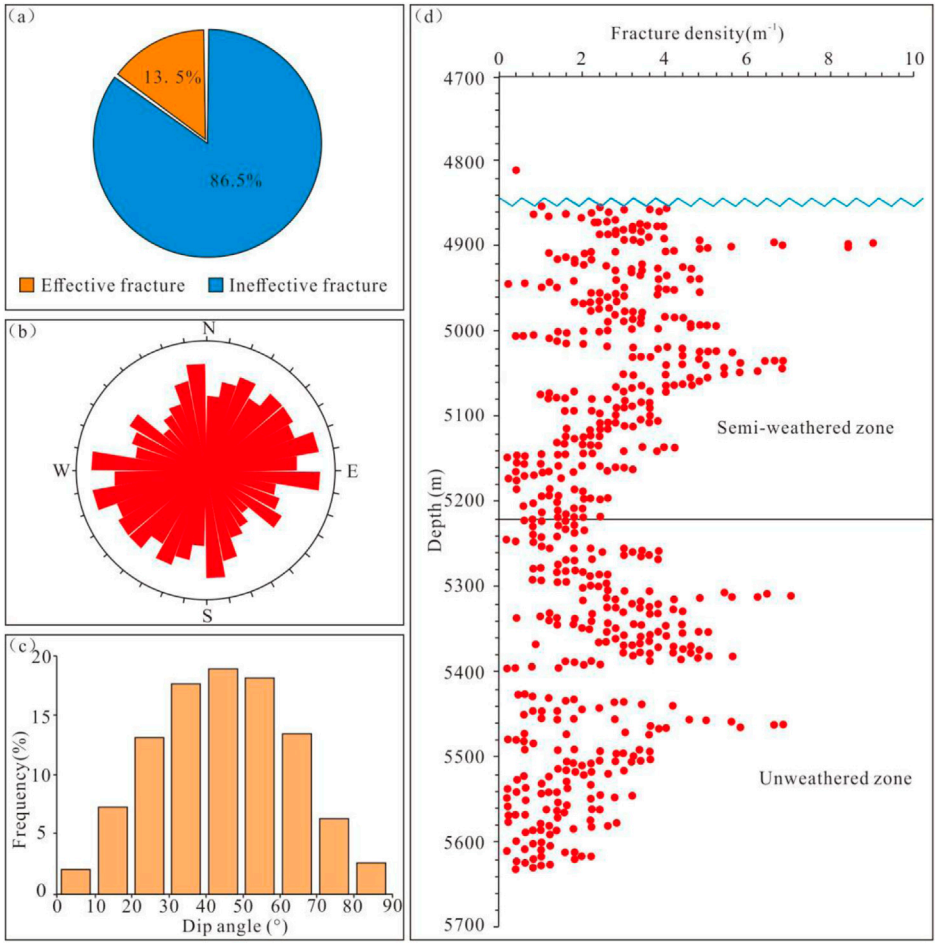

FIGURE 4
Quantitative characterization of fracture parameters and fracture distribution on imaging log. **(A)** Pie chart of fracture effectiveness. **(B)** Rose diagram of fracture strikes. **(C)** Diagram of dip angle distribution. **(D)** Fracture intensity and distribution in vertical.

average of 53.0 m/m^2, and it is up to 93 m/m^2 at local position (Figure 5C). The value of structural fractures is about 10–30 m/m^2, with an average of 20.1 m/m^2. These fractures are highly filled by mudstone, iron and a small amount of calcite, where 68% of weathering fractures are completely filled, 15% are half filled, 17% are not filled, and thereby only 32% are effective fractures (Figure 5D).

Discussion

The Bozhong 19-6 buried-hill reservoirs were developed at early stage and experienced multiple and complex geological events at later stage, resulting in strong heterogeneity in natural fracture distribution. Investigation on weathering crusts and fault zones on outcrops and fracture distribution at underground as well as another data shows that nature fracture development at buried-hill reservoirs in the study area is mainly controlled by lithology, weathering crusts, faults and ancient landform, etc.

Lithology

Lithology is the primary factor regulating fracture development under the same tectonic stress (Gong et al., 2019b; Lyu et al., 2019; Gong et al., 2021a; Cao et al., 2021; Gong et al., 2022), since mechanical properties of rocks vary as a function of mineral compositions, structures and textures. The influence of lithology and mineral compositions on fracture development was analyzed based on similar outcrops, cores and thin sections. Fractures are well developed at six lithologies in the study area, e.g., cataclasite, with a linear density of 43.46 m^{-1}, followed by metamorphic granite and granite gneiss, while they are poorly developed at rocks with

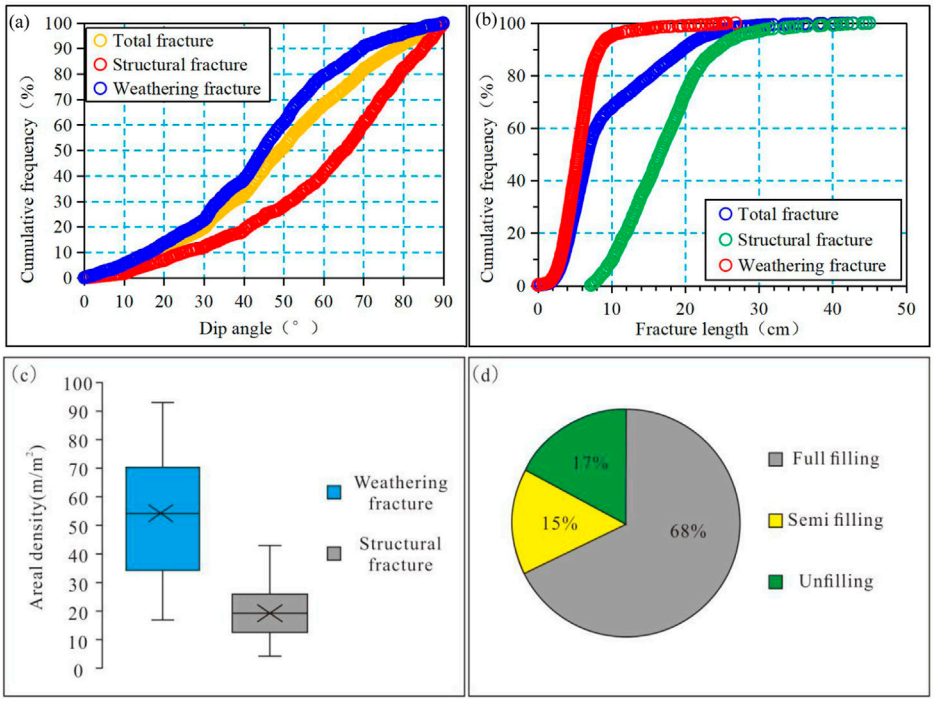

FIGURE 5
Quantitative characterization of fracture parameters and fracture distribution on cores. **(A)** Dip angle of fracture. **(B)** Fracture length. **(C)** Fracture intensity. **(D)** Fracture effectiveness.

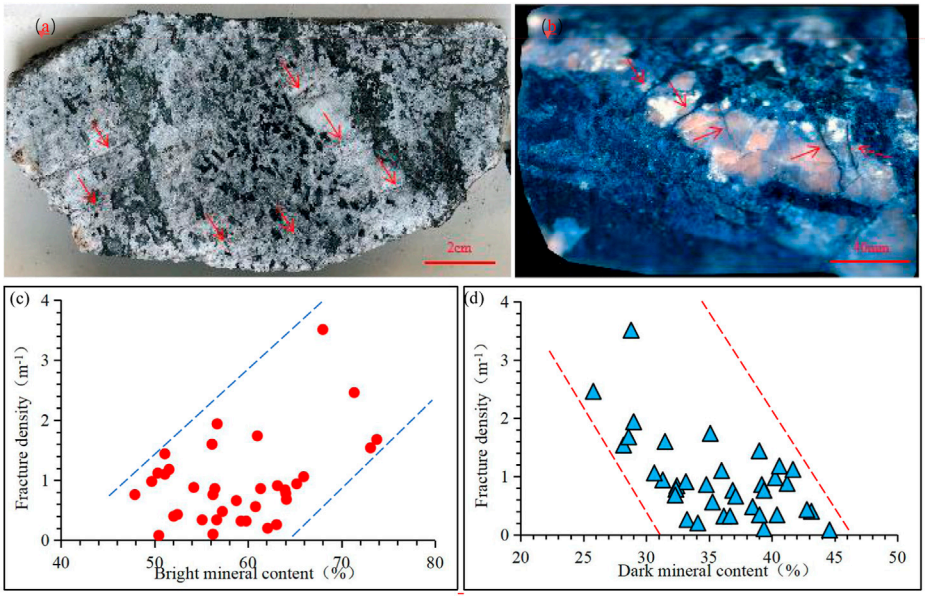

FIGURE 6
Controlling of lithology on fracture distributions. **(A,B)** Variation in fracture development with mineral types. **(C)** Relationship between bright mineral contents and fracture development. **(D)** Relationship between dark mineral contents and fracture development.

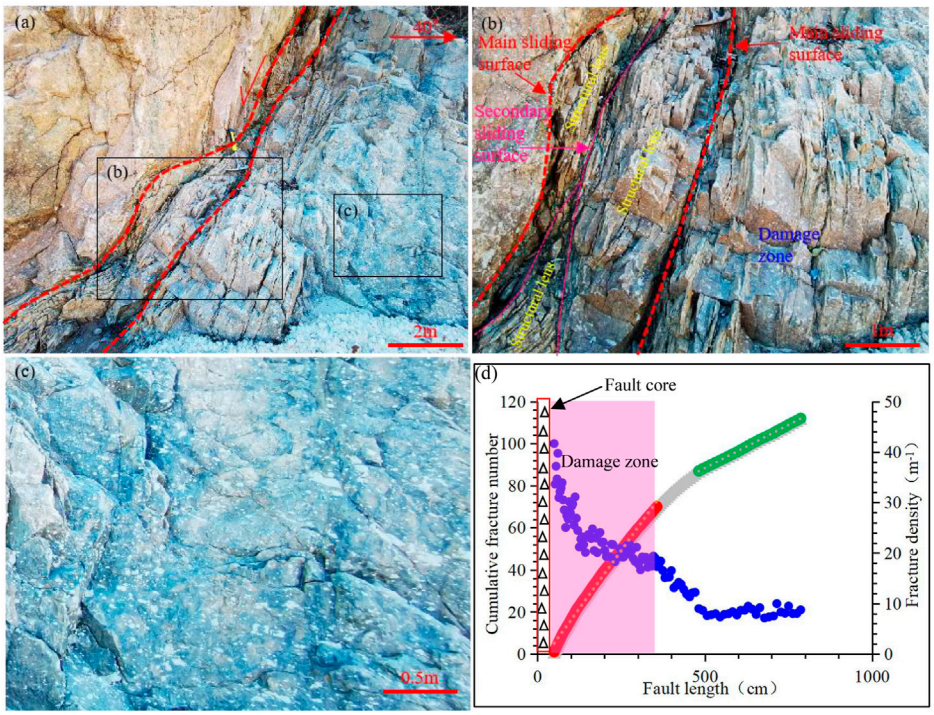

FIGURE 7
Internal structure of fault zone at Gushiyu village. **(A)** The overall characteristics of Gushiyu fault; **(B)** characteristics of the fault core; **(C)** characteristics of fracture development in the host rock; **(D)** distribution characteristics of fractures near faults.

high dark mineral content, e.g., amphibole and pyroxene, with linear density of 6.65 m^{-1}.

Mineral compositions are important elements to determine fracture development under the same geological conditions (Wang et al., 2022). Samples from outcrops and cores show that, fractures are mainly developed in rocks with high bright mineral contents (quartz, feldspar, etc.), with density up to 40-50 m^{-1}) (Figure 6). These fractures generally terminate abruptly at the boundary between light and dark minerals, and only a small number of large structural fractures pass through this boundary. Ductile deformation is commonly occurred to the units with high dark mineral content (biotite, hornblende, etc.), where fractures are poorly developed, with density less than 5 m^{-1}. The comparison between mineral contents derived from XRD analysis and fracture development shows that the bright mineral contents are significantly positively correlated with fracture development, whereas the dark mineral contents are negatively correlated with fracture development (Figure 6).

Fault structure

Faults those can regulate stress distribution at different structure units (Gong et al., 2021b; Ferrill et al., 2021; Zeng et al., 2022) *via* stress disturbance can significantly control fracture development at metamorphic buried-hill reservoirs. Generally, obvious stress concentration along faults can enhance fracture development. Considerable previous studies confirm that fault system is characterized by a dual structure that can be divided into two units, i.e., fault core and damage zone (Zeng et al., 2022; Gong et al., 2021b; Peacock et al., 2017). The fault core is generally composed of sliding surface, fault gouge, breccia, structure lens and cataclasite, and the damage zone is composed of fractures and secondary faults with different scales (Choi et al., 2016). Figure 7 shows a typical fault at metamorphic rocks at the Gushiyu village in the north of Qinhuangdao city. The hanging wall is dominated by sandstone and the footwall is slate or schist. It is a normal fault with occurrence of 165°∠80°and displacement of 8–10 m.

Fault core and damage zone can be identified from this fault system. The core is 10–50 cm in thickness, mainly composed of primary sliding surface, secondary sliding surface and structure lens. The structure lens are large in scale, with size of 0.25 m×2.0-0.1 m×0.3 m. Fractures in the structure lens are well developed, with density up to 30–40 m/m^2. The fault core is an open one with no fillings, which can act as a predominant seepage channel. Fractures are densely developed near the sliding surface, with average density of 20–30 m/m^2 and fracture spacing as low as

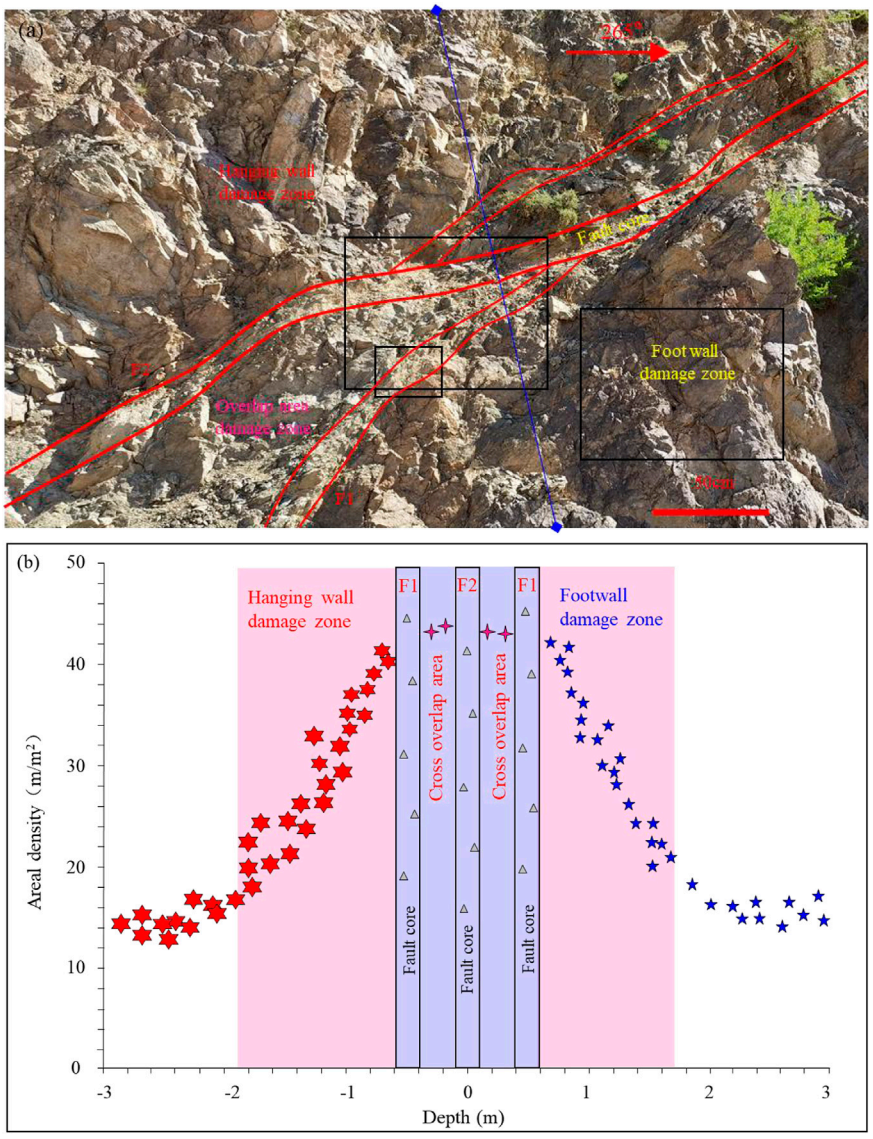

FIGURE 8
Fault structure and distribution of associated fractures at Huoqing Road. **(A)** The overall characteristics of Huoqing Road fault; **(B)** internal structure of fault zone and distribution of associated fractures.

1–2 cm. Two groups of fractures are developed in the damage zone. One group is parallel to the sliding surface, with small fracture spacing and high density, while another group is at an angle of 75° with the sliding surface, which has large fracture spacing (10–30 cm). They are intersected to form a fracture network with good connection. Another two groups of fractures occur far from the sliding surface (Figure 7), where they are weakly developed, with spacing of 30–40 cm and density of 3–5 m/m^2. The width of the damage zone can be identified when the fracture density is consistent with the regional fracture density. Relationship between distance and cumulative fracture numbers suggests that it is about 3.48 m for the Gushiyu fault.

The damage zone can be divided into tip damage zone, wall damage zone and linkage damage zone based on its location (Kim and Sanderson, 2010; Choi et al., 2016; Luo et al., 2018; Zhu et al., 2021). The tip damage zone refers to the subseismic faults and fractures at the end of faults, also known as process zone. Wall damage zone is distributed on two sides of sliding surface. The linkage damage zone is developed at the position where two or more faults are interacted with each other, e.g., fault intersection or overlapping zone. Figure 8 shows two faults at the Huoqing Road of Wulate, Bayannur City, Inner Mongolia, where F1 fault was developed at early stage and was cut by F2 fault. The dual structure with similar core

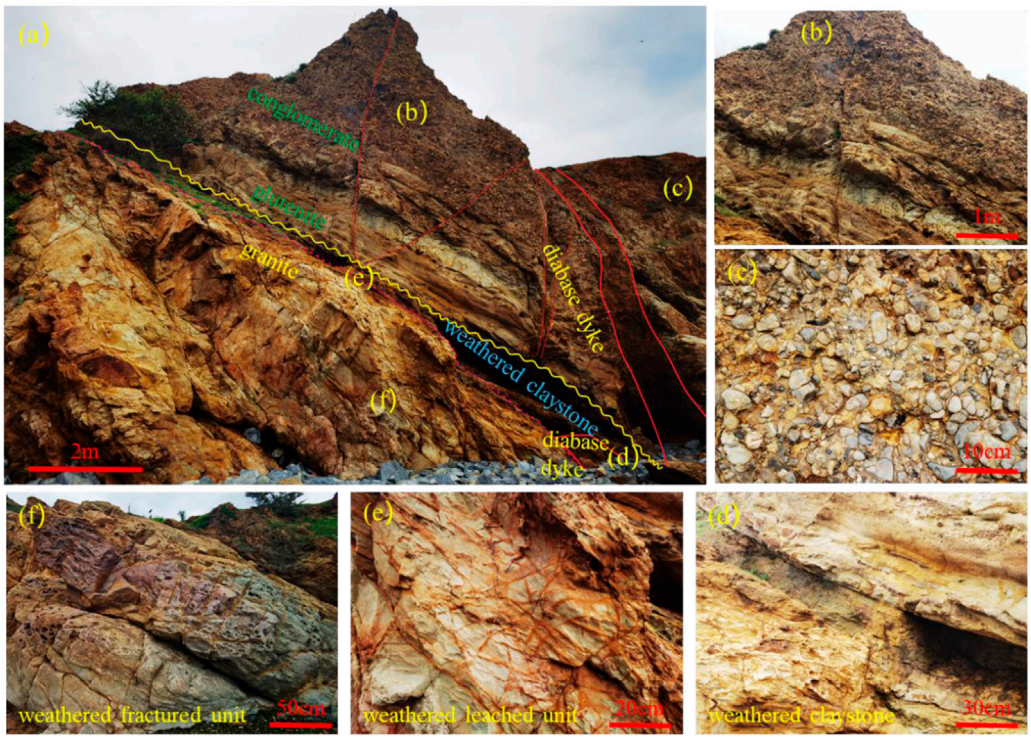

FIGURE 9
Paleo-weathering crust structure and fracture distribution at Longhuitou scenic spot. **(A)** Overall characteristics of weathering crust and fractures; **(B)** fracture characteristics in glutenite; **(C)** fracture characteristics in conglomerate; **(D)** fracture characteristics in weathered claystone; **(E)** fracture characteristics in semi-weathered leached unit; **(F)** fracture characteristics in semi-weathered fractured unit.

structures can be observed from both these two faults, including fault breccia and a small amount of fault gouge. F1 is a normal fault with occurrence of 195°∠48°, core width of 10–20 cm and displacement of 1.2 m F2 is also a normal fault with occurrence of 206°∠53°, core width of 20–30 cm and displacement of 1.5 m. Fractures are well developed at damage zone, especially at positions overlapped by these two faults, where multiple sets of fractures are interacted to form networks, with density up to 40 m/m^2. The density decreases to about 10 m/m^2 with increasing distance from the fault, and thereby, the identified width of the damage zone is 0.8–1.5 m.

Weathering crust structure

Structures of two paleo-weathering crusts were described in detail to clarify fracture distribution in vertical at metamorphic buried-hill reservoirs. The first weathering crust is located at the top of the Archaeozoic granite at Longhuitou scenic spot, Xingcheng City, Liaoning Province, and is overlaid by the Middle Jurassic Haifanggou polymict conglomerate. It can be divided into weathered claystone, semi-weathered leached unit and semi-weathered fractured unit based on weathering degree and fracture development (Figure 9). The weathered claystone is 20–30 cm in thickness. Most was converted into brownish-red and loose clay minerals under intensive weathering and erosion with weak fracture development, where the structure and texture of the parent rock were completely destroyed. Some claystone was washed away by rain or sea water to form grooves. The semi-weathered leached unit remains original mineral framework under general weathering and leaching, where both weathering fractures and structural fractures can be observed. The weathering fractures have extremely high density, with an average of 30–50 m/m^2, as a result, fracture networks can be formed with length of 10–30 cm, indicating high-quality seepage channel. Both sides of fractures are iron red, with a width of 3–6 cm. Structural fractures and weathering fractures were developed at the semi-weathered fracture unit. However, different from semi-weathered leached unit, it is dominated by structural fractures, with low density but large scale (meter-scale). Trans-gravel fractures, gravel-edge fractures and intra-gravel fractures can be found at overlaid sandy conglomerates, where the trans-gravel fractures are mainly large-scale shear ones (3–6 m in length). However, fracture density is significantly lower than that of three units at weathering crust.

FIGURE 10
Paleo-weathering crust structure and fracture distribution at Jiashan. **(A)** Overall characteristics of weathering crust and fractures; **(B)** fracture characteristics in gravelly sandstone; **(C)** fracture characteristics in weathered claystone; **(D)** fracture characteristics in weathered broken unit; **(E)** fracture characteristics in semi-weathered leached unit; **(F)** fracture characteristics in semi-weathered fractured unit.

The second paleo-weathering crust is situated at the top of Archaeozoic granite at Jiashan, Xingcheng City, Liaoning Province, which is overlaid by the Changzhougou gravelly coarse sandstone of the Changcheng System. The weathering crust can be divided into weathered claystone, weathered broken unit, semi-weathered leached unit and semi-weathered fractured unit (Figure 10). The weathered claystone, which is dominated by soil-like secondary minerals, is 15–25 cm in thickness. Part of the claystone was washed by rain to form grooves. The weathered broken unit is mainly composed of cataclasite and mudstone, with high argillaceous content. Strong weathering and dissolution resulted in vaguely-visible fracture networks, where fractures were obviously dissolved with smooth surface. Weathering fractures and structural fractures were developed at the semi-weathered leached unit, while the former was popular, with an average density of 30–50 m/m^2 and length of 10–30 cm. Minerals are difficult to be identified in this unit because of strong weathering and dissolution, with abundant dissolution pores and enlarged fractures. Most fractures are not filled and are widened by dissolution, with uneven surfaces and dissolution pores at local positions. As a result, fracture network is developed with good connection. Structural fractures and weathering fractures were developed at the semi-weathered fractured unit, with low density but large size, commonly in meter-scale. The overlaid gravelly coarse sandstone intervals are dominated by strata-bounded fractures and through-strata fractures of tectonic-origin.

Therefore, a well-developed weathered crust can be divided into weathered claystone, weathered broken unit, semi-weathered leached unit, semi-weathered fractured unit and unweathered unit (Kim and Sanderson, 2005; Hou et al., 2013; Chen et al., 2021; Fan et al., 2021) (Figure 11). The weathered claystone is typical compacted rock with no fracture. From the weathered broken unit to the unweathered unit, fracture types change from weathering ones to structure ones, with decreasing fracture density. Factors affecting unit thickness and fracture development are lithology, weathering period and weathering degree of the bedrock as well as ancient landform.

Ancient landform

Weathering and leaching, playing an important role in controlling weathering crust structure and vertical zoning of

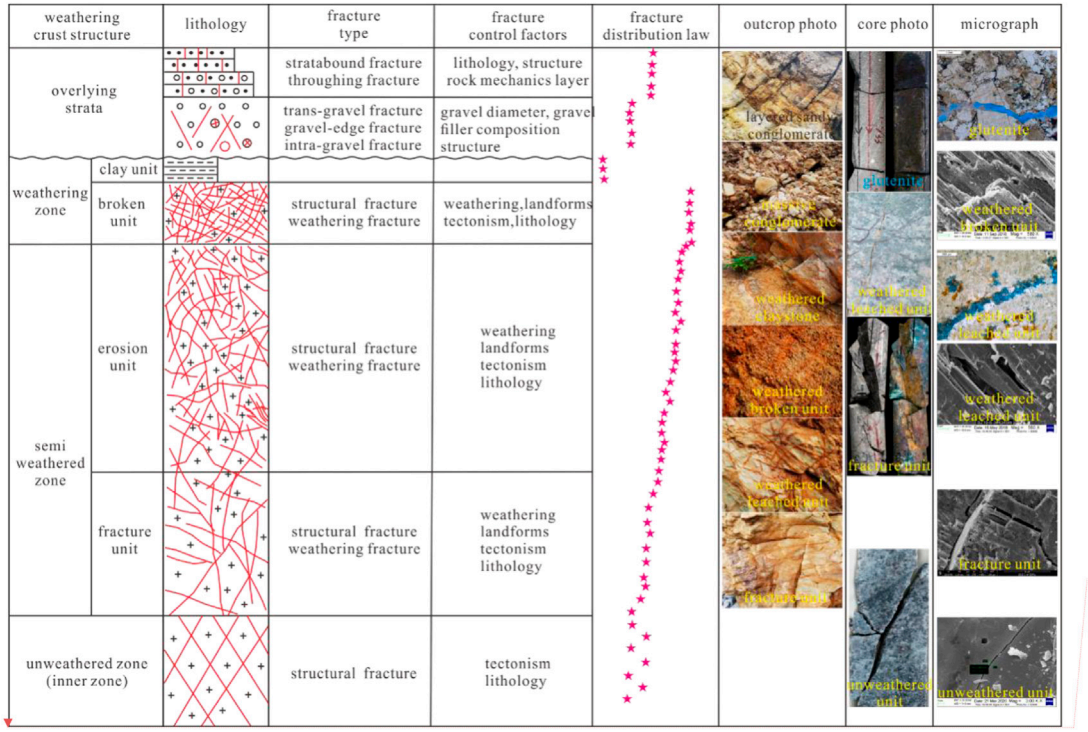

FIGURE 11
Weathered crust structure pattern and fracture distribution in vertical.

reservoirs, are depended on ancient landform (Zou et al., 2011; Zeng et al., 2017). Exploration activities show that new and thin strata above buried hills are good indicators of high positions, where long-term weathering and leaching can contribute positively to high-quality reservoir development. The location of ancient landform also affects fracture types and fracture development. Structural fractures, extensional fractures associated with stress releasing under gravity and weathering fractures can be developed at the high of the landform, especially at high mountains with large slopes. The former two are large in extension and cutting depth, up to hundreds of meters, providing channels for weathering and leaching. The latter is small in scale, but have large density, up to 50–100 m/m^2. These fractures are commonly well connected, contributing to strong weathering and leaching. Weathering fractures and structural fractures can be developed at small ridges and steep slopes, where weathering fractures are popular, cutting rocks into fragments and promoting weathering and leaching. Structural fractures are popular at most gentle slopes covered by sediments, e.g., colluvium and slope wash, with a few weathering fractures, where weathering and leaching are relatively weak. Weathering is also weak at gully that is covered by flowing water or sediment throughout the year, but faults can be well developed, especially structural fractures. Sedimentation is the primary geological event at low positions, where no significant weathering and leaching are developed.

Conclusion

Structural fractures, weathering fractures and dissolution fractures are developed at metamorphic buried-hill reservoirs in the study area, where structural fractures and weathering fractures are the most popular ones. Fracture types vary greatly among different structure positions. Four fracture groups were mainly developed in the study area, i.e., NEE-SWW trending, near EW trending, near NS trending and NW-SE trending. Oblique fractures are prevailing with dip angle of 30°–60°, with bedding-parallel fractures and subvertical fractures of secondary importance. The fracture density identified by imaging log is about 1–5 m^{-1}. Vertically, the overall fracture density at the semi-weathered unit is higher than that in the unweathered unit, and multiple fractures are also developed in the unweathered unit. Fractures are well developed yet are significantly filled on cores, especially in the weathering unit, where areal density of weathering fractures is about 30–70 m/m^2, with an average of 53.0 m/m^2. The areal density of structural fractures is mainly distributed at 10–30 m/m^2, with an average of 20.1 m/m^2.

Lithology, fault, weathering crust and ancient landform are primary elements governing fracture distribution. Fracture density is high in lithology with high bright mineral contents. Faults have a typical dual structure including fault core and

damage zone. The fracture density decreases with increasing distance from faults. Damage zone will be ended when the density is consistent with the regional fracture density. The width of the damage zone is generally determined by factors, e.g., fault scale and structure location. The semi-weathered leached unit is dominated by well-developed and well-connected weathering fractures, with structural fractures of secondary importance. Different from that, the semi-weathered damage zone is dominated by structural fractures, followed by weathering fractures, with low fracture density. Structural fractures are prevailing at the unweathered unit, where fracture density is high for certain lithology at local positions. Ancient landform primarily controlled the distribution of weathering fractures, which were well developed at high positions (e.g., ridges and slopes), while sedimentation was the primary geological event at gentle slopes and low positions.

Data availability statement

The original contributions presented in the study are included in the article/supplementary material, further inquiries can be directed to the corresponding author.

Author contributions

LM: conceptualization; TF: writing—review and editing; HF: writing—review and editing; TN: formal analysis, visualization; LG: writing–original draft; XS: investigation; YS: supervision; YC: investigation.

Funding

This study is financially supported by National Natural Science Foundation of China (Grant No. 42072155), Natural Science Foundation of Heilongjiang Province (Grant No. YQ 2022D006) and Postdoctoral Research Foundation of Heilongjiang Province (Grant No. LBH-Q21001).

Conflict of interest

LM, TF, HF, and TN were employed by CNOOC Research Institute Ltd., China.

The remaining authors declare that the research was conducted in the absence of any commercial or financial relationships that could be construed as a potential conflict of interest.

Publisher's note

References

Cao, D., Zeng, L., Lyu, W., Xu, X., and Tian, H. (2021). Progress in brittleness evaluation and prediction methods in unconventional reservoirs. *Petroleum Sci. Bull.* 1, 31–45. doi:10.3969/j.issn.2096-1693.2021.01.003

Chen, X., Wei, A., Wang, Y., Gao, S., Ye, T., and Li, X. (2018). Controlling effect of archaean metamorphic rocks on fractures in southwest Bohai Sea. *Geol. Sci. Technol. Inf.* 37, 165–173. doi:10.19509/j.cnki.dzkq.2018.0223

Chen, X., Zhao, Z., Hui, G., Yue, J., and Zhao, J. (2021). Characteristics of weathered metamorphic rocks crust in bohai sea and its quantitative prediction. *Mar. Geol. Front.* 37, 33–41. doi:10.16028/j.1009-2722.2020.168

Choi, J., Edwards, P., Ko, K., and Kim, Y. (2016). Definition and classification of fault damage zones: A review and a new methodological approach. *Earth-Science Rev.* 152, 70–87. doi:10.1016/j.earscirev.2015.11.006

Deng, Y. (2015). Formation mechanism and exploration practice of large-medium buried-hill oi fields in Bohai Sea. *Acta Pet. Sin.* 36, 253–261. doi:10.7623/syxb201503001

Dou, L., Wei, X., Wang, J., Li, J., Wang, R., and Zhang, S. (2015). Characteristics of granitic basement rock buried-hill reservoir in Bongor Basin, Chad. *Acta Pet. Sin.* 36, 897–904. doi:10.7623/syxb201508001

Fan, T., Niu, T., Fan, H., Wang, S., Xiao, D., and Luo, J. (2021). Geological model and development strategy of Archean buried hill reservoir in BZ19-6 condensate field. *China Offshore Oil Gas* 33, 85–92. doi:10.11935/j.issn.1673-1506.2021.03.009

Ferrill, D., Smart, K., Cawood, A., and Morris, A. (2021). The fold-thrust belt stress cycle: Superposition of normal, strike-slip, and thrust faulting deformation regimes. *J. Struct. Geol.* 148, 104362. doi:10.1016/j.jsg.2021.104362

Gao, S., Zeng, L., Ma, S., He, Y., Gong, L., Zhao, X., et al. (2015). Quantitative prediction of fractures with different directions in tight sandstone reservoirs. *Nat. Gas. Geosci.* 26, 427–434. doi:10.11764/j.issn.1672-1926.2015.03.0427

Gong, L., Cheng, Y., Gao, S., Gao, Z., Feng, J., Wang, H., et al. (2022). Fracture connectivity characterization and its controlling factors in the Lower Jurassic tight sandstone reservoirs of eastern Kuqa. *Earth Sci.*. doi:10.3799/dqkx.2022.066

Gong, L., Fu, X., Wang, Z., Gao, S., Jabbari, H., Yue, W., et al. (2019). A new approach for characterization and prediction of natural fracture occurrence in tight oil sandstones with intense anisotropy. *Bulletin* 103, 1383–1400. doi:10.1306/12131818054

Gong, L., Gao, M., Zeng, L., Fu, X., Gao, Z., Gao, A., et al. (2017). Controlling factors on fracture development in the tight sandstone reservoirs: A case study of jurassic-neogene in the kuga foreland basin. *Nat. Gas. Geosci.* 28, 99–208.

Gong, L., Gao, S., Liu, B., Yang, J., Fu, X., Xiao, F., et al. (2021). Quantitative prediction of natural fractures in shale oil reservoirs. *Geofluids* 2021, 1–15. doi:10.1155/2021/5571855

Gong, L., Liu, B., Fu, X., Jabbari, H., Gao, S., Yue, W., et al. (2019). Quantitative prediction of sub-seismic faults and their impact on waterflood performance: Bozhong 34 oilfield case study. *J. Petroleum Sci. Eng.* 172, 60–69. doi:10.1016/j.petrol.2018.09.049

Gong, L., Wang, J., Gao, S., Liu, B., Miao, F., Meng, Qi., et al. (2021). Characterization, controlling factors and evolution of fracture effectiveness in shale oil reservoirs. *J. Petroleum Sci. Eng.* 203, 108655. doi:10.1016/j.petrol.2021.108655

Gong, L., Zeng, L., Chen, S., Gao, S., Zhang, B., Zu, K., et al. (2016). Characteristics of micro-fractures and contribution to the compact conglomerate reservoirs. *Geotect. Metallogenia* 40, 38–46. doi:10.16539/j.ddgzyckx.2016.01.004

Hou, M., Cao, H., Li, H., Chen, A., Wei, A., Chen, Y., et al. (2019). Characteristics and controlling factors of deep buried-hill reservoirs in the BZ19-6 structural belt, Bohai Sea area. *Nat. Gas. Ind.* 39, 33–44. doi:10.3787/j.issn.1000-0976.2019.01.004

Hou, L., Luo, X., Wang, J., Yang, F., Zhao, X., and Mao, Z. (2013). Weathered volcanic crust and its petroleum geologic significance: A case study of the carboniferous volcanic crust in northern xinjiang. *Petroleum Explor. Dev.* 40, 257–265. doi:10.11698/PED.2013.03.01

Hu, Z., Xu, C., Yang, B., Huang, Z., and Su, W. (2017). Reservoir forming mechanism of Penglai 9-1 gra nite buried-hills and its oil geology significance in Bohai Sea. *Acta Pet. Sin.* 38, 274–285. doi:10.7623/syxb201703004

Huang, J., Tan, X., Cheng, C., Li, Z., Ma, L., Zhang, H., et al. (2016). Structural features of weathering crust of granitic basement rock and its petroleum geological significance: A case study of basement weathering crust of dongping area in qaidam basin. *Earth Sci.* 41, 2041–2060. doi:10.3799/dqkx.2016.528

Kim, Y., and Sanderson, D. J. (2005). The relationship between displacement and length of faults: A review. *Earth-Science Rev.* 68, 317–334. doi:10.1016/j.earscirev.2004.06.003

Kim, Y., and Sanderson, D. (2010). Inferred fluid flow through fault damage zones based on the observation of stalactites in carbonate caves. *J. Struct. Geol.* 32, 1305–1316. doi:10.1016/j.jsg.2009.04.017

Luo, Q., Fariborz, G., Zhong, N*., Wang, Y., Qiu, N., Skovsted, C. B., et al. (2020). Graptolites as fossil geo-thermometers and source material of hydrocarbons: An overview of four decades of progress. *Earth-Science Rev.* 200, 103000. doi:10.1016/j.earscirev.2019.103000

Luo, Q., George, S., Xu, Y., and Zhong, N. (2016). Organic geochemical characteristics of the mesoproterozoic hongshuizhuang formation from northern China: Implications for thermal maturity and biological sources. *Org. Geochem.* 99, 23–37. doi:10.1016/j.orggeochem.2016.05.004

Luo, Q., Gong, L., Qu, Y., Zhang, K., Zhang, G., and Wang, S. (2018). The tight oil potential of the Lucaogou Formation from the southern Junggar Basin, China. *Fuel* 234, 858–871. doi:10.1016/j.fuel.2018.07.002

Luo, Q., Zhang, L., Zhong, N., Wu, J., Goodarzi, F., Sanei, H., et al. (2021). Thermal evolution behavior of the organic matter and a ray of light on the origin of vitrinite-like maceral in the Mesoproterozoic and Lower Cambrian black shales: Insights from artificial maturation. *Int. J. Coal Geol.* 244, 103813. doi:10.1016/j.coal.2021.103813

Luo, Q., Zhong, N., Qin, J., Li, K., Zhang, Y., Wang, Y., et al. (2014). Thucholite in Mesoproterozoic shales from northern north China: Occurrence and indication for thermal maturity. *Int. J. Coal Geol.* 125 (1), 1–9. doi:10.1016/j.coal.2014.01.009

Lyu, W., Zeng, L., Zhou, S., Du, X., Xia, D., Liu, G., et al. (2019). Natural fractures in tight-oil sandstones: A case study of the upper triassic yanchang formation in the southwestern ordos basin, China. *Bulletin* 103, 2343–2367. doi:10.1306/0130191608617115

Peacock, D., Dimmen, V., Rotevatn, A., and Sanderson, D. (2017). A broader classification of damage zones. *J. Struct. Geol.* 102, 179–192. doi:10.1016/j.jsg.2017.08.004

Wang, D., Wang, Q., Liu, X., Zhao, M., Hao, Y., and YiWei, H. (2019). Characteristics and developing patterns of gneiss buried hill weathering crust reservoir in the sea area of the Bohai Bay basin. *Acta Petrol. Sin.* 35, 1181–1193. doi:10.18654/1000-0569/2019.04.13

Wang, J., Hu, C., Pan, Y., Huang, Q., Yuan, H., Gong, L., et al. (2022). Fracture development characteristics and comprehensive evaluation of buried hill metamorphic reservoir in Jihua 1 area. *Chin. J. Geol.* 57, 463–477. doi:10.12017/dzkx.2022.027

Wang, X., Zhou, X., Xu, G., Liu, P., Gao, K., and Guan, D. (2015). Characteristics and controlling factors of reservoirs in Penglai 9-1 large-scaleoilfield in buried granite hills, Bohai Sea. *Oil Gas. Geol.* 36, 262–270. doi:10.11743/ogg20150211

Xie, h. (2020). Gas resources and accumulation model of BZ19-6 Archean buried-hill large-scale gas reservoir in Bozhong Sag, Bohai Bay Basin. *Pet. Geol. Exp.* 42, 858–866. doi:10.11781/sysydz202005858

Xu, C., Du, X., Liu, X., Xu, W., and Hao, Y. (2020). Formation mechanism of high-quality deep buried-hill reservoir of Archaean metamorphic rocks and its significance in petroleum exploration in Bohai Sea area. *Oil Gas. Geol.* 41, 235–247. doi:10.11743/ogg20200201

Xu, C., Yu, H., Wang, J., and Liu, X. (2019). Formation conditions and accumulation characteristics of Bozhong 19-6 large condensate gas field in offshore Bohai Bay Basin. *Petroleum Explor. Dev.* 46, 27–40. doi:10.1016/s1876-3804(19)30003-5

Xue, Y., Wang, Q., Niu, C., Miao, Q., Liu, M., and Yin, J. (2020). Hydrocarbon charging and accumulation of BZ 19-6 gas condensate field in deep buried hills of Bozhong Depression, Bohai Sea. *Oil Gas. Geol.* 41, 891–902. doi:10.11743/ogg20200501

Ye, T., Niu, C., Wang, Q., Dai, L., and Li, F. (2021). Characteristics and controlling factors of large bedrock buried-hill reservoirs in the bohai Bay Basin—A case study of the BZ19-6 condensate field. *Acta Geol. Sin.* 95, 1889–1902.

Zeng, L., Gong, L., Guan, C., Zhang, Be., Wang, Q., Zeng, Q., et al. (2022). Natural fractures and their contribution to tight gas conglomerate reservoirs: A case study in the northwestern sichuan basin, China. *J. Petroleum Sci. Eng.* 210, 110028. doi:10.1016/j.petrol.2021.110028

Zeng, L., Zhao, X., Zhu, S., and Zhao, J. (2017). Waterflood-induced fractures and its significance for development of low-permeability sandstone oil reservoirs. *Petroleum Sci. Bull.* 3, 336–343. doi:10.3969/j.issn.2096-1693.2017.03.031

Zeng, L., Zhu, R., Gao, Z., Gong, L., and Liu, G. (2016). Structural diagenesis and its petroleum geological significance. *Petroleum Sci. Bull.* 2, 191–197. doi:10.3969/j.issn.2096-1693.2016.02.015

Zhou, X., Wang, Q., Feng, C., Ye, T., Liu, X., Hao, Y., et al. (2022). Formation conditions and geological significance of large Archean buried hill reservoirs in Bohai Sea. *Eart. Scie.* 47, 1534–1548. doi:10.3799/dqkx.2021.249

Zhou, X., Xiang, H., Yu, S., Wang, G., and Yao, C. (2005). Reservoir characteristics and development controlling factors of JZS Neo-Archean metamorphic buried hill oil pool in Bohai Sea. *Petroleum Explor. Dev.* 2005, 17–20.

Zhou, X., Zhang, R., Li, H., Wang, B., and Guo, Y. (2017). Major controls on natural gas accumulations in deep-buried hills in Bozhong Depression, Bohai Bay Basin. *J. China Univ. Petroleum* 41, 42–50. doi:10.3969/j.issn.1673-5005.2017.01.005

Zhu, H., Song, Y., and Tang, X. (2021). Research progress on 4-dimensional stress evolution and complex fracture propagation of infill wells in shale gas reservoirs. *Petroleum Sci. Bull.* 3, 396–416. doi:10.3969/j.issn.2096-1693.2021.03.032

Zou, C., Hou, L., Tao, S., Yuan, X., Zhu, R., Zhang, X., et al. (2011). Hydrocarbon accumulation mechanism and structure of large-scale volcanic weathering crust of the Carboniferous in northern Xinjiang, China. *Sci. China Earth Sci.* 41, 221–235. doi:10.1007/s11430-011-4297-8